Unusual secondary-electron-emission spectra: Surface-exciton sources for Si(111)7×7

P. E. Best
Physics Department and Institute of Materials Science, University of Connecticut, Storrs, Connecticut 06269-3136
(Received 24 February 1992; revised manuscript received 29 June 1992)

In many respects electron-beam excited secondary-electron-emission spectra (SEES) from the (111)7×7 surface of 10-Ω cm *n*-type silicon are like those from metals: The maximum in the secondary current is observed within a few eV of the threshold, and, with negative potential (with respect to chamber ground) applied to the sample, V_s, the spectra retain their shape while their detected kinetic energy increases by eV_s. The shapes of SEES from 10-Ω cm *p*-type samples are different in a gross qualitative way: Secondary currents for kinetic energies out to 8 eV above threshold are greatly reduced, with the maximum in the distribution occurring at a kinetic energy of about 12 eV above threshold. With negative potential applied to the sample the shape of the spectra change, until at a value of V_s of about -12 V the shape observed for the *n*-type samples is recovered. With more negative values of V_s this part of the SEES retains its shape, while its detected kinetic energy increases by eV_s, again just like those for metals. In addition to these electrons, for $-12 < V_s < -300$ V another group of secondary electrons is observed to emerge from the sample, but from outside the beam landing area, and with energies close to chamber ground. The observation of secondary-electron emission at two distinct energies indicates that under these conditions this silicon surface is a nonequipotential surface. A model for all of these observations is presented in terms of mobile surface excitons, whose existence was previously demonstrated from angle-resolved energy-loss spectra. These long-lived excitons consist of a selvedge electron bound to a surface-state hole; the selvedge region lying between the bulk crystal and the image potential. A mode of formation of these surface excitons is postulated; electrons impinging on the surface from within the crystal, with energies greater than 1.5 eV above the bottom of the conduction band, can be captured by surface holes to form surface excitons. The unusual SEES is associated with the surface being *p* type. Bombardment of the (111)7×7 surface of *p*-type silicon by electrons with energies between 40 and 300 eV is an effective way of producing long-lived surface excitons. It is suggested that this technique constitutes a source which can produce surface excitons for study by other probes. There is evidence for the formation of surface excitons in scanning tunneling, and in inverse photoemission spectra.

I. INTRODUCTION

The spectra discussed here are of the low-energy ($E < 20$ eV) secondary electrons which emerge from a silicon (111)7×7 surface under bombardment by a higher-energy ($E > 40$ eV) electron beam. The field of electron-beam excited secondary electron emission spectra (SEES) is sufficiently established to have associated with it a standard model to describe the gross spectral features. It is a three-step model: excitation, followed in turn by transport, and emergence into the vacuum.[1] The excitation step is mainly by plasmon formation, as can be verified by studying the energy-loss spectra (ELS) of the sample. The transport starts from the decay of the plasmons into single-particle states. The resulting energetic electrons and holes in turn excite electron-hole pairs in a cascade process until the excess energy is dissipated. Electrons from the resulting distribution which impinge normally on the surface with sufficient energy are transmitted to the vacuum with a probability which approaches unity for energies greater than about 0.3 eV above the vacuum level. This model was established from considerations of SEES from metallic samples, although it is used for other samples as well. Its main prediction is the shape and amplitude of SEES.

In contrast with the situation for metals, the investigation of SEES from single-crystal silicon is a subject in its infancy. Since the ready availability of ultrahigh-vacuum (UHV) systems in the early 1960s, I can find just seven papers on SEES from the silicon (111)7×7 surface,[2–8] compared with the 25 papers on photoemission spectra from that surface.[9] For *n*-type samples of 5-Ω cm resistivity, and for takeoff angles within 50° of the normal, the SEES are accounted for by the standard model. SEES from the (111)7×7 surface of *p*-type silicon have not been reported before.

The angle-resolved SEES reported here are for a range of doping corresponding to bulk resistivities of between 5-Ω cm *n*-type and 10-Ω cm *p*-type. Spectra from the 5- and 10-Ω cm (low-resistivity) *n*-type samples are the same as reported previously.[5–7] However, with increasing ease, samples of bulk resistivity from 100-Ω cm *n*-type to 10-Ω cm *p*-type show three features which cannot be explained by the standard model. For the case of minimum electric field between sample and chamber, the secondary current is reduced compared to that from low-resistivity *n*-type samples. With increasing negative sample bias, relative to chamber ground, the shape of the SEES changes dramatically, which is not the case for the low-resistivity *n*-type samples; and for a range of negative sample bias relative to chamber ground, the appearance of certain features in SEES indicates that there are two

 ©1992 The American Physical Society

regions of different electric potential at the surface. The observations are sufficiently unexpected that I have done considerable checking of them, and the validity of the results is beyond doubt insofar as I can do the same experiment sequentially on n- and p-type samples, respectively. The tests I have done rule out systematic errors such as those due to stray electric or magnetic fields, or due to nonsample emission.

The work described here is primarily experimental. However, the results do conform to the predictions of a model. The strengths of the model are that it qualitatively describes the whole range of unusual SEES in a consistent manner, and that it quantitatively accounts for the energies of peaks in SEES. The model contains features which are unusual, at least for surfaces. This is to be expected, as by definition unusual data require for their explanation a model that is out of the ordinary. These features include the production of long-lived surface excitons by the capture of electrons by surface holes, and the transport of energy by surface excitons. Predictions have been made from the model so that it can be tested.

Section II of the paper is experimental, in which details of the apparatus and method are described. Results and discussion follow in Sec. III. The data are basically of two kinds. The main results are SEES which are unusual in that they cannot be interpreted in the same way as spectra from metals or from low-resistivity n-type silicon. The interpretation of these data requires a more complicated model than the standard one, and this model is presented later. Along with the main results are ancilliary measurements, ELS and Auger spectra. Where the interpretation is straightforward these data are discussed along with its presentation. Subsections in Sec. III include one on the validity of the data, in which those aspects of the results most relevant to establishing validity are collected. The model is presented and discussed in Sec. IV. Relevant background information from the literature concerning the electronic structure of the (111)7×7 surface, including surface excitons, is first described. The model is presented and discussed in two parts, one quantitative and one qualitative. Predictions from the model are made, and other measurements which show the effects of surface exciton production are discussed. A summary and conclusions are presented in Sec. V.

II. EXPERIMENT

Two different apparatus have been used in these experiments, although in the same low-magnetic-field ultrahigh-vacuum (UHV) chamber. Apparatus 1 and the chamber and pumping system have been described before.[10] The same magnetic shielding has been employed for both apparatus, attenuating the field to less than 7 mG over the scattering region. With this field it is predicted that electrons with energies of less than 0.25 eV can travel from the sample to the entrance aperture of the spectrometer with less than 1° deviation, a prediction verified in operation.[5]

While apparatus 1 was versatile in allowing angles both of incidence and takeoff to be varied independently, it was cumbersome to align and use, so apparatus 2 was constructed. In this apparatus the gun, spectrometer, and sample holders are all bearing mounted on a stainless-steel U frame (Fig. 1), in turn bolted to the chamber. The inside dimension of the U is 19 cm. Rotations of the electron gun and the spectrometer supports are effected by manual rotary-motion UHV feedthroughs joined to the axles of the loads by leaf-spring couplings. These axles share a common axis, XX' of Fig. 1, which is referred to as the principal axis. The use of an angular scale outside of the vacuum chamber is not optimum for accurate angular measurements. Once backlash is removed, angular displacements are repeatable to within 0.5°. Alignment of the components, so that the mechanical axes of the gun and the spectrometer both intersected the center of the sample surface perpendicular to the principal axis, was done mechanically while the apparatus was outside the chamber. Each electron-optic axis and its corresponding mechanical axis are not necessarily colinear. Deflector plates at the exit of the gun were used to effect final alignment, using low-energy electron-diffraction (LEED) and SEES features as monitors.

The sample was held in place by two tantalum clips, one at each end of the 19×4×0.3-mm wafers. The clips were constructed so that the principal axis of the apparatus was parallel to, and at the front surface of, the sample. In general, the desired atomic planes are not precisely parallel to the polished surface of a wafer, so a small corrective rotation must be applied to the sample to align the atomic planes to the principal axis. That was effected by mounting the sample goniometer support arm on an axle (axis Y of Fig. 1) whose orientation was also controlled by a rotary-motion feedthrough. The coupling to this axis is by a key at the end of a rotary-feedthrough drive, which fitted into a keyway in the drive shaft of the goniometer support. The sample azimuthal angle (measured about axis Z of Fig. 1) was driven by a wire-connected coupling (part a of Fig. 1). This arrangement gives sufficient flexibility to permit rotations of ±1° about the Y axis. These alignment facilities are necessary to repeat the earlier published results, for which precise coplanar alignment of incident beam, takeoff direction, and a high-symmetry crystal plane are required. The present

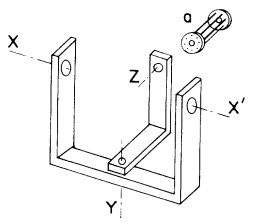

FIG. 1. The support frame for the electron gun and spectrometer for angle-dependent measurements of SEES and ELS. The spectrometer and gun holders share axis XX', while the crystal, whose surface lies in XX', is supported on a bearing whose axis is collinear with Z. Part a is a wire-connected coupling.

SEES results can be reproduced easily without such precise alignment.

The spectrometer consists of a hemispherical analyzer preceded by a lens of the same type as used previously.[11] The angular divergence of electrons passing from the analyzer to the channeltron electron multiplier detector was limited to 5°, in order to minimize the detection of stray electrons scattered from the walls of the analyzer. The analyzer was run at pass energies E_p of between 4 and 25 eV, and had an intrinsic resolution (dE/E_p) of 0.03, and a mean radius of 2.5 cm. The angular acceptance of the analyzer was constant for most electron energies. The spectrometer case potential was that of the chamber ground. Secondary electrons with kinetic energy relative to the chamber ground, E, of less than the chosen pass energy must be accelerated into the spectrometer by the action of the entrance lens. In that case it is found that the overall collection efficiency changes with E. It is relatively easy to measure this efficiency and to correct for it.[10] The collection angle for low-energy electrons gives a viewing circle at the sample surface of between 4 and 6 mm, depending on the ratio of the spectrometer pass energy to the kinetic energy relative to chamber ground. The sample clips are well out of view of the spectrometer. LEED measurements were made for all surfaces for which SEES are reported, except for those from the oxide-covered surface. Observed LEED patterns were consistent with a silicon (111)7×7 surface. Analog detection of the current from the Channeltron electron multiplier using a Keithley picoammeter was utilized for all samples. Pulse detection was also used for measurements on the 1500-Ω cm n-type sample.

The electron gun was similar in form to that used in apparatus 1. Oxide cathodes were used in both apparatus. The cathode was replaced for each pumpdown, requiring bakeout before and after cathode activation. The overriding advantages of the oxide cathode are its low power requirement (<1.5 W) and the low filament current it needs (<0.25 A). The size of the electron-beam spot is calculated to be 0.5 mm, a value verified by measuring the sample current as the beam is swept across the edge of the sample, using the sample width (4 mm) to calibrate the deflection system. The maximum current reaching the sample in both apparatus was 0.3 μA, although lower currents were sometimes utilized. The lower currents were obtained by applying negative bias to the grid electrode of the electron gun at constant filament current. Depending on beam current and energy, diffraction spots had a full width at half maximum (FWHM) of from 0.75° to 1.5°.

The silicon (111)7×7 surface is one of the few surfaces that can be cleaned by heating in UHV. Wafers were chemically cleaned by the method described by Henderson.[12] After installing in the chamber, an ultraviolet/ozone treatment was used prior to pumpdown.[13] Heating in UHV at 1170 K for 15 min then produced a well-defined 7×7 LEED pattern. This procedure gives ELS which are characteristic only of the clean surface.

When measuring SEES of low-resistivity n-type samples the sample potential is adjusted so that the electric field between the sample and spectrometer is minimized. For the value of V_s which eliminates the electric field between sample and spectrometer, the emitted electrons will move to the spectrometer entrance and be detected without serious distortion of the SEES. For V_s more negative by ΔV_s, all secondary electrons will be detected with an energy larger than before by $e\Delta V_s$, where e is the electron charge; the shape of the distribution will be unchanged, and the spectra will be observed at an energy larger by $e\Delta V_s$. For positive ΔV_s, electrons with energy above the silicon vacuum level by an amount less than $e\Delta V_s$ will not reach the spectrometer. The shape of SEES will be changed. These effects are demonstrated in Fig. 7 of Ref. 10. The procedure for finding the minimum field is then clear: measure SEES as a function of V_s, and choose the most positive V_s for which the spectral shape is unchanged. If spectra only at normal emergence are to be measured, then a value of V_s more negative than the field-free value will not cause distortion of the spectra. For angle-dependent measurements in a system without hemispherical symmetry about the sample, however, the minimum value electric field should be used. If the work functions of the sample and the spectrometer case, respectively, are the same, a value of $V_s=0$ would give rise to a field-free region. The magnitude of the measured value of V_s to achieve the field-free condition has consistently been less than 1.5 V in both apparatus.

In both apparatus 1 and 2 an instrument artifact that cannot be eliminated has been observed. For increasingly negative V_s at takeoff angles close to the surface normal the SEES are detected at higher values of E, as described above. Ideally in those cases no current should be detected at energies below the threshold step of SEES. In fact an artifact is observed at low kinetic energies in the spectra from the low-resistivity n-type samples. The asymmetric feature is broad (~6 eV width) and structureless; its amplitude is small compared with that of any feature discussed here or previously, and decreases monotonically with more negative V_s. It is probable that the electrons contributing to this feature are stray secondaries emerging from the region of the spectrometer case around the entrance aperture.

III. RESULTS AND DISCUSSION

A. Results

Energy levels for the experiment are represented in Fig. 2(a), where Fermi levels, work functions (W), and applied potentials (V) between the chamber ground, cathode (c), and sample (s) are shown. The main spectral features observed for low-resistivity n-type silicon samples are shown schematically in Fig. 2(b); the abrupt threshold preceding the low-energy peak of secondary electrons is at energy "D" from the elastic peak, where

$$D=eV_c+W_c-eV_s-W_s\ , \tag{1}$$

where D is accurate to within the sample band gap [1.1 eV (Ref. 14)] plus the cathode thermal energy. I refer to

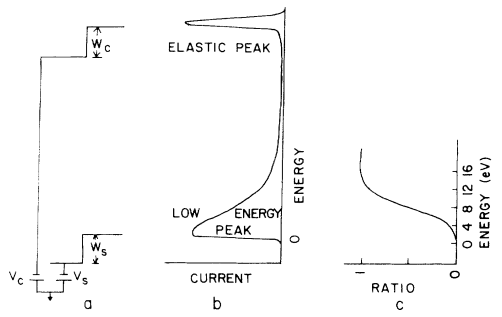

FIG. 2. (a) Energy-level diagram showing the work functions (W), applied potentials (V), Fermi levels, and vacuum levels of the sample (subscript s) and cathode (subscript c). (b) Schematic energy spectrum of electrons emerging from a sample which is bombarded by electrons from the cathode, showing the peak of elastically scattered electrons, and the low-energy peak of secondary electrons. The threshold of the low-energy peak is normally observed at an energy "D" from the elastic peak [Eq. (1)]. (c) Ratio of reduced spectrum to standard SEES for the (111)7×7 surface of p-type silicon. The current at the low-energy region of the reduced SEES is greatly attenuated.

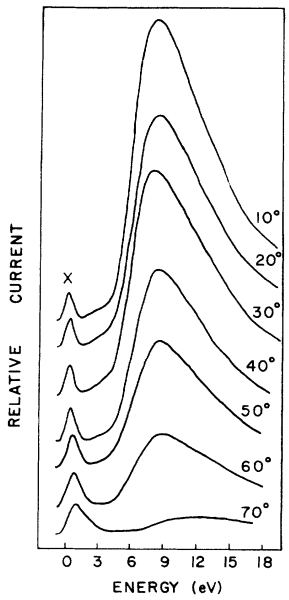

FIG. 3. SEES from (111)7×7 surface of 10-Ω cm p-type silicon, for variable takeoff angle relative to the surface normal (indicated), for constant input beam conditions: 56 eV at a polar angle of 20°, at an azimuthal angle not coincident with a high-symmetry direction of the crystal. Unless otherwise indicated, all spectra in the one figure were recorded with identical gain settings for detected current.

this shape as standard. The work functions of the oxide cathode and the silicon (111)7×7 surface are 1.8 and 5.3 eV, respectively.[15,16]

Measured SEES from n-type samples with 5- and 10-Ω cm resistivities showed only standard shape in both apparatus, for all beam currents used. I will describe results from 10-Ω cm p-type, 1.5-k Ω cm n-type, and 100-Ω cm n-type samples, in that order.

1. 10-Ω cm p-type samples

SEES from two 10-Ω cm p-type samples were measured in apparatus 2, with measurements of a 10-Ω cm n-type sample interspersed between these. A typical series of SEES for $V_s=0$ as a function of the takeoff angle is shown in Fig. 3, where the energy scale refers to the kinetic energy relative to the leading edge of the low-energy peak labeled X. At $V_s=0$ this zero of the energy scale happens to be at the vacuum level of the silicon (±1.1 eV) as judged from the energy of the elastic peak and Eq. (1). For all values of V_s the zero of the energy scale used in displayed SEES is consistent with the energy of the vacuum level of the spectrometer case. The spectra are not of standard shape. At $E=0$ eV is a small peak labeled X that persists to all angles of emergence with little change of intensity. Where the broad maximum of the SEES is normally seen for low-resistivity n-type samples [Fig. 2(b)], for values of E from 0 to about 10 eV, there is little current. The intensity of the broad peak at about 10 eV has an angular dependence that can be associated with emission from bulk states, unlike peak X, whose angular dependent intensity is consistent with a surface origin.

With increasing negative values of V_s, at constant V_c-V_s, the SEES develop as shown in Figs. 4 and 5. I will describe separately the development of the broad maximum and the X peak, respectively. Little change is seen in the broad peak for V_s down to −6 V, at which point a definite threshold step appears at an energy of 6 eV in the original spectra (too small to be shown in Fig. 4). The energy of this threshold step is just where the threshold of the spectra for a low-resistivity sample would be for these conditions, according to Eq. (1). With more negative V_s the amplitudes of both the threshold step and the peak increase until at $V_s=-12$ V the standard shape is recovered (Fig. 4). I refer to that potential as V_r. For this sample values of V_r between −6 and −17

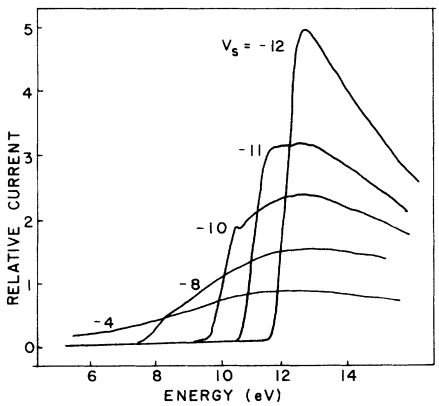

FIG. 4. SEES from p-type silicon for V_s from −4 to −12 V for input beam conditions: constant V_c-V_s of 72 V at an angle of 30° to the normal. The SEES were recorded at a normal takeoff angle. The standard shape was recovered at $V_s=-12$ V in this case.

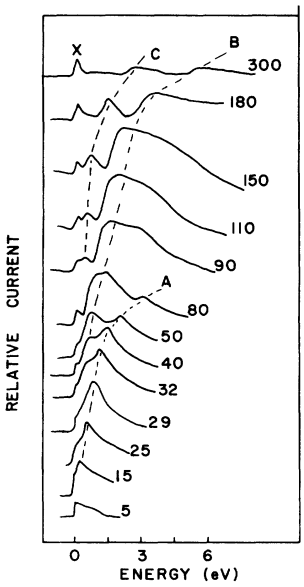

FIG. 5. Development of SEES from a 10-Ω cm p-type sample with application of negative V_s, showing the low-energy end of the spectrum. The negative of the applied value of V_s is shown alongside each spectrum. These spectra were recorded at normal takeoff for constant $V_c - V_s = -300$, and an incident polar angle of 30° from the normal.

V were recorded, the lowest value being for the most negative V_c used, −300 V. With more negative V_s the shape of the peak remains constant for as far as I followed it, $V_s = -150$ V. Because the broad peak for $V_s < -12$ V has a standard shape I interpret the shape of the SEES for $0 > V_s > -12$ V as an indication that there is a considerable reduction in secondary current for those conditions. I refer to SEES with a reduction of current as "reduced" spectra. An estimate of the magnitude of the reduction of the secondary current was made by taking the ratio of the current at $V_s = 0$, ignoring the intensity in the X peak to that at $V_s = -18$ V for one series of spectra. That ratio has the shape of a broad step, reaching unity at $E = 13$ eV [Fig. 2(c)].

On the other hand, peak X did not change much for $0 > V_s > -12$ V, for the spectra shown in Fig. 5, for which $V_c - V_s$ was constant at −300 V. At $V_s = -12$ V the intensity of the X peak increased suddenly, and a new peak labeled A in Fig. 5 "emerged" from peak X. With more negative V_s the energy of A increased, although the intensity began to fall until it was no longer observed at $V_s = -90$ V. In turn, with increasingly negative V_s, peaks B and C emerged from peak X. While series A and C have a well-defined "peak" appearance, B features have complex shape for $-45 > V_s > -160$ V, subsequently having step shape. Limitations of the apparatus prevented these measurements for $V_s < -300$ V. The energy of the leading edge of peak X did not vary as V_s changed from 0 to −300 V, although the breadth of the peak varied from 0.2 to nearly 2 eV.

The shape of the SEES from this sample did not vary with sample current, I_s, down to 2×10^{-9} A. At $V_s = 0$ the shape of the X peak varied with incident-beam angle and landing energy, although that phenomenon was not systematically investigated. For incident-beam energies of less than 20 eV only the elastic and some loss peaks were consistently observed, secondary emission not being excited strongly.

It is possible that there are as many secondary electrons actually emitted for the $V_s = 0$ case as for $V_s = -12$ V (Fig. 4), but that they are not detected because of deflection by fields within the chamber. I cannot measure the secondary yield (current out/current in) in this chamber, but by monitoring the sample current for $V_s = 0$ as a function of V_c the value of V_c at which the secondary-emission yield goes through unity can be determined as follows. The landing energy of the incident beam, eV_c, for which the yield goes through unity for the first time is called E_{I}, for the second, E_{II}.[17] For $eV_c < E_{\mathrm{I}}$ a net electron flux enters the sample, while for $E_{\mathrm{I}} > eV_c < E_{\mathrm{II}}$ a net flux leaves the sample. The first change of direction of the sample current as a function of V_c indicates when $eV_c = E_{\mathrm{I}}$. For many incident-beam conditions used in this work with low-resistivity n-type samples, E_{I} is found to be about 130 eV, close to the literature value.[18] For native-oxide-covered surfaces of both p- and n-type 10-Ω cm samples a value of E_{I} of between 58 and 80 eV was measured. For the clean (111)7×7 surface of 10-Ω cm p-type samples the value of E_{I} is greater than 500 V, definitely indicating that the secondary yield is lower for the (111)7×7 surface of the p-type sample, in agreement with the observed reduced spectra.

The sample holder to sample contact is a metal-semiconductor junction, at best. While the beam currents used were below normal diode reverse-bias current levels, it was prudent to check whether there is a potential change at the surface between conditions giving rise to the reduced and the standard spectra, respectively. The detected energy of Auger spectra from surface and near-surface atoms includes all potential changes from sample clip to surface atoms, and thus can be used to probe for potential changes. It is mentioned that the energy of Auger spectra are independent of the sample work function. For fixed $V_c - V_s$, silicon LVV Auger spectra were measured for two values of V_s: one gave reduced SEES like that for $V_s = -4$ in Fig. 4; the other giving SEES of standard shape, like the $V_s = -12$ V case in Fig. 4. The Auger spectra were measured at a takeoff angle of 20° to the normal, in an undifferentiated mode. No significant difference was observed between the spectra; there is less than 0.3-V difference in the potential of surface atoms between the two cases.

Electrons contributing to the X peak, always observed at close to zero kinetic energy relative to the spectrometer case, can come only from a region of the surface at zero potential, with no field between the emitting region and the spectrometer. Peak X was observed at the same time as the standard SEES, which had a threshold step at the energy expected for a surface at potential V_s, for V_s down to −300 V. I conclude that there are two regions of different electric potential on this surface for these

conditions. Again, Auger spectra are sensitive to the potential at the emitting atoms, so Auger spectra were searched for with $V_s = -120$ V, $V_c = -300$ V. Si LVV Augers were observed at an energy appropriate for a surface at -120 V, but not for a surface region at ground potential. The nonobservation of Auger electrons from a region at ground potential for $V_s = -120$ V indicates that the $V=0$ region of the surface lies outside of the landing area of the incident beam.

For one of the p-type samples, SEES were measured after a preliminary sample heating to 800 °C for 10 min. This heating is not sufficient to remove the thin oxide layer formed in the chemical cleaning process, and no LEED pattern was observed for this sample condition. For this oxide-covered sample SEES of standard shape were observed with a threshold step at energy D from the elastic peak, as predicted by Eq. (1) for a 0.3-μA incident-beam current and a variety of input angles. The breadth of the threshold step was slightly greater than that for the clean surface. In both scanning electron microscopy,[19] where the signal is derived from secondary electrons, and in photoemission,[20] it has been observed that a thin oxide layer is essentially transparent to electrons emerging from the underlying silicon. That apparently is what occurs in secondary emission from this sample also. From a comparison of these SEES with those from the clean sample it can only be concluded that the SEES features of nonstandard form, i.e., reduced spectra and peaks X, A, B, and C, are associated with surface processes. For all incident-beam conditions that were used surface and volume plasmon losses were observed in ELS measurements, for $V_c < -40$ V.

2. 1.5-k Ω cm n-type sample

Measurements on this sample were made only in apparatus 2. Reduced spectra and X, A, B, and C peaks were all observed for $I_s = 0.3$ μA for incident-beam angles within 35° of the surface normal, for beam conditions which did not give strong diffraction peaks. For similar $V_c - V_s$, however, V_r was always less negative for this sample than for the p-type sample. That is, the standard shape was more readily recovered.

Variation of SEES with incident-beam current was observed for this sample for normal emergence. The spectra tended toward standard shape as the current was reduced, although the difference between the extreme spectra of Fig. 6 is associated with a hundredfold decrease in current.

By observing the LEED pattern I could monitor whether the incident-beam conditions were appropriate for a Bragg maximum or for other strong diffraction effects. For incident-beam conditions that did not give rise to strong diffraction effects a consistent dependence of the shape of SEES on the incident angle was observed. The SEES tended to standard shape as the incident polar angle changed from normal toward grazing incidence (Fig. 7). In the absence of strong diffraction effects it can be assumed that this observation means that the SEES tend to standard shape as the direction of the primary beam within the sample changes away from the surface normal.

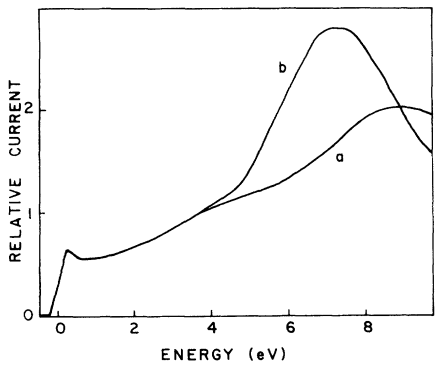

FIG. 6. Spectra showing the shape dependence of SEES on the incident-beam current for the 1500-Ω cm n-type sample, measured at a normal takeoff angle, for an incident beam of 55 eV at a polar angle of 33°. The signals have been normalized at the low-energy step: it is the change of shape which is significant. The beam currents were 10^{-9} A for the a curve, 10^{-11} A for the b.

For incident-beam conditions that did give rise to strong diffraction effects a consistent dependence of SEES on the incident polar angle was not observed; sometimes the SEES tended to standard shape with an increase of polar angle away from the surface normal, as above, but the opposite trend was also observed.

The model presented later predicts that a 3-eV peak should be observed in the ELS of this sample. An extensive search was made, culminating in the only result in this paper which requires precise alignment for its reproduction. The ELS were recorded with a relatively low-energy beam, 15 eV, using as the effective primary beam

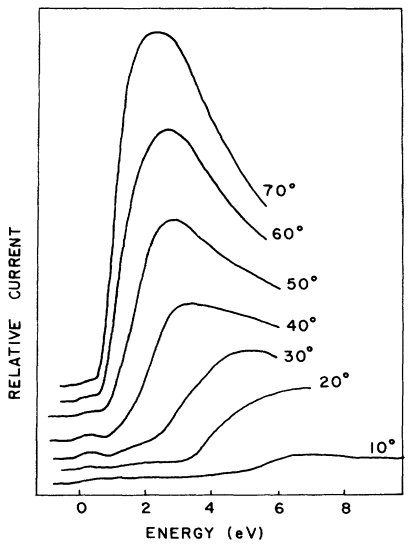

FIG. 7. SEES from the 1500-Ω cm n-type sample as a function of the input angle (indicated) in an arbitrary azimuth, for $V_s = 0$, $V_c = -70$ V. The takeoff angle was 20° from the surface normal. There is a dramatic change of shape as the angle of incidence changes to grazing incidence.

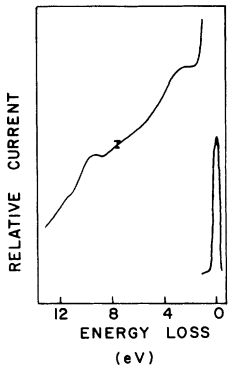

FIG. 8. Energy-loss spectrum for a 15-eV beam incident at 65° in the $[\bar{2}11]$ azimuth. The outgoing specular beam was the effective primary beam which maximized the observed loss peaks at $dk_{\parallel}=0$. The error bar represents the peak-to-peak noise amplitude. In all other spectra presented the noise level is less than twice the thickness of the drawing line. Losses of 3.0±0.4 and 9.3±0.4 eV are observed, both more than 1 eV wide. The loss region of the spectrum is amplified by a factor of 100 compared to the elastic peak.

the (0,0) specular beam, emerging at an angle of 65° from the normal in the $[2\bar{1}\,\bar{1}]$ azimuth. Two broad loss peaks are observed, at 3.0±0.4 and 9.2±0.4 eV, respectively (Fig. 8).

For normally incident electrons the angle of detection of the (1,0) diffraction spot in the $[2\,\bar{1}\,\bar{1}]$ azimuth of the 7×7 pattern was followed down to $V_c=-1.5$ V, for $V_s=0$ V. In all cases the angle of detection agreed with the expected outgoing angle to within experimental error, ±1.5°. This measurement rules out stray magnetic fields as a possible perturbing influence on the SEES.

3. 100-Ω cm n-type sample

Measurements were made on this sample in apparatus 1. Reduced spectra and the X peak were observed only for the maximum beam current (0.3 μA) and for a very limited range of incident angles of the exciting beam. In that case spectra similar to those in Fig. 3 were recorded. For a beam current of 1×10^{-8} A only features reported earlier for the low-resistivity sample were observed.[5–7]

B. Validity

There are two features of the SEES which are unexpected, and require validation beyond the usual care taken with the apparatus construction and the measurements. The features are the reduced current spectra and peaks X, A, B, and C. For the clean samples the LEED pattern was used as monitor to establish the beam focus condition for all measurements. This ensured that the incident beam was properly focused and was striking the sample near its center for all recorded SEES. The observation of diffraction maxima at angles corresponding to the well-documented LEED patterns assured that there were no gross fields in the chamber. However, the secondary electrons have much lower energy than the elastically scattered electrons, so other measurements were made to ensure the validity of the SEES.

The shapes of the SEES in question were independent of analyzer pass energy, which rules out possible problems within the lens-analyzer system. The question then becomes whether stray fields were present to deflect secondary electrons from the spectrometer entrance aperture so as to cause the reduced spectra at low values of V_s, and to deflect stray secondaries toward the entrance aperture at more negative values of V_s to give rise to peaks X to C. Stray fields are discussed below.

The possible presence of an unexpected magnetic field was ruled out by the LEED measurement at $V_c-V_s=-1.5$ V. However, electric fields could arise from the arrival of highest energy electrons at an electrically isolated surface, to cause an electric field that disturbs the lower- but not the higher-energy electrons. That source of stray field is more difficult to rule out as a possible disturbance. Routine measurements before each pumpdown ensured that no major parts exposed to the electron beam were electrically floating. Almost identical reduced spectra and the X peak were observed for samples in the two different apparatus. It is improbable that this could be the result of coincidental random malfunctions.

The value of E_1 measured for the p-type sample, >500 eV, indicates a greatly reduced secondary current from that sample, independent of any fields in the chamber, in agreement with the observed reduced spectra.

Consider the spectra labeled −8 V in Fig. 4. A threshold step is observed at the energy predicted by Eq. (1), indicating that electrons of this energy from the beam landing area reach the detector. Why would not all the other electrons of the same energy observed in the −12-V spectrum of Fig. 4 be observed? Certainly no macroscopic field in the scattering region can disperse the electrons in a manner to cause this. The SEES in that figure do not change with small deflections of the incident beam across the sample surface.

For similar incident-beam conditions the p-type sample covered with a native oxide emitted SEES of standard shape; SEES from clean (111)7×7 surfaces were unusual in the manner shown in Figs. 3–5.

Samples of 10-Ω cm resistivity were loaded in the chamber in the order p type, n type, p type. Input beam conditions similar to those that gave unusual results for both p-type samples gave standard spectra for the n-type sample. The data for the n-type sample establish the proper operation of the apparatus, and those for the p-type samples establish the reproducible nature of the data for the p-type samples. The unusual SEES arise from the silicon (111)7×7 surface itself.

IV. THE MODEL

A. Background

Critical to the interpretation of the SEES reported here is the established existence of excitons at this surface. A brief summary of the evidence for this exciton follows.

Angle-resolved photoemission results indicate the existence of a flat band of surface states just below the Fermi level.[9] SEES from n-type silicon show a series of quasistationary states located in the selvedge region of the sample,[5,7] between the crystal interior and the image potential. These states extend from an energy 2.5 eV below to at least 6 eV above the vacuum level.

The 1.9-eV peak in the ELS was first observed by Rowe and Ibach, who showed that it is associated with transitions from a dangling-bond surface state.[21] The angular dependence of the intensity of this loss peak shows that the associated process has $\Delta k_{\parallel}=0$.[22-25] It was further observed that this peak occurred just below a band which I associated with the excitation of a dangling-bond electron to selvedge states. With these assignments the 1.9-eV loss peak must be due to the excitation of a surface exciton, a selvedge electron bound to a surface hole.[22] The electron in this exciton is bound by 2.9 ± 0.3 eV below the vacuum level, although the binding within the exciton relative to the bottom of the band of the free-electron-like selvedge states is 0.4 eV. That the exciton is derived from the continuum of selvedge states, rather than the vacuum continuum, clearly distinguishes it from image states.

For incident-beam energies less than 100 eV it has been demonstrated that the shape of angle-resolved SEES and angle-resolved ELS can depend considerably on incident-beam angle and energy,[5-7,22] although a detailed study of that dependence has not been made. Because of this the comparison of results obtained by different workers is really only meaningful if they are for the same input beam conditions, or if enough input beam conditions have been investigated so that "all" types of spectra are observed.

Further background is required for a discussion of reduced spectra and peaks X, A, B, and C. A first approximation to the charge distribution in an electron-irradiated sample can be deduced from a knowledge of the excitation, transport, and emergence steps. An incident electron with energy greater than about 40 eV excites plasmons in low-momentum transfer collisions,[26-28] ending up as a hot free carrier in the conduction band.[29] From the decay of plasmons and the subsequent cascade Coulomb scattering,[1,30] there will be a sheath of electron-hole pairs extending along the path from the surface to the free carriers. Electrons emerging into the vacuum will change this distribution by leaving an excess of holes at the surface. Silicon has surface states below the Fermi level in the band gap,[9] so the excess holes can be trapped as surface holes. An electron-irradiated surface will, therefore, tend to be more p type than the ground state. I will call a surface with an excess of holes a p surface; an n-type sample can have a p surface. The fate of surface holes is a concern of this paper.

For a beam incident perpendicular to the surface the carrier distribution might look like that in Fig. 9(a), with considerable separation between the hot free carriers and the trapped surface holes. I have used mean free path information for silicon[27-29] to show that this sheath would have a thickness t of about 600 A for a 300-eV normally incident beam. It is emphasized that apart from the incident electron and the excess hole left by an electron emerging into the vacuum, equal numbers of electrons and holes are formed by the incident beam.

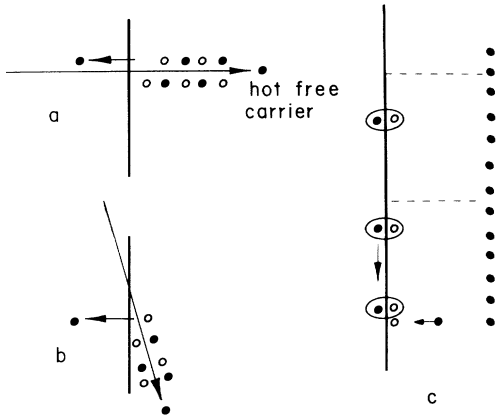

FIG. 9. Illustrations depicting various aspects of models described in the text. A solid dot, a circle, and an ellipse represent an electron, a hole, and an exciton, respectively. (a) A normally incident electron leaving a trail of electron-hole pairs before becoming a hot free carrier in the bulk. In this case a secondary electron has been emitted, leaving an excess hole at the surface. (b) An electron at close to grazing incidence. In this case the hot free carrier is much closer to the surface. Remembering that the beam width is much greater than the range of the incident electrons, it can be seen that the free electron and the surface hole are in close proximity in this case, in contrast to the situation depicted in (a). (c) The dotted lines define the limits of the beam landing area. Excitons are formed in this area and migrate to where they are trapped by a surface hole. The field associated with this hole accelerates a bulk electron toward the surface, where it emerges into the vacuum, ionizing an exciton in the process. The emerging electrons are detected as peaks X, A, B, and C, as described in detail in the text.

B. The model

I suggest that the unusual SEES features reported here are the indirect results of a surface which has an excess of holes, without specifying whether the holes are intrinsic or the result of secondary electron emission as described above. The presence of surface holes can lead to surface exciton formation other than by direct excitation as in ELS, as follows. Some of the hot electrons moving toward the surface have energies matching those of states near the bottom of the selvedge band.[5,14] Electrons can be diffracted from bulk to a selvedge state, subsequently being trapped by a surface hole to form a surface exciton. The small value of the basic reciprocal-lattice vectors on this reconstructed surface is conducive to such diffraction from states in many regions of bulk k space. Surface exciton formation will always be a possible mode of elimination of bare surface holes in a secondary-electron-emission experiment on this surface.

Peaks X, A, B, and C are discussed first; it is only for these that the model is quantitative. It was argued above that peaks X, A, B, and C are due to electrons which emerge from a region of the surface at chamber ground

potential, with no field between this region and the spectrometer case. However, there is still the potential V_s between the sample clips and chamber ground. For the region responsible for peaks A to C this potential drop must be within the sample. This indicates that there must be a positive surface charge at the region of the surface at ground potential. I suggest a model for peaks X, A, B, and C which contains a means for depositing positive surface charge outside the beam landing area.

The energy dependence of peaks A, B, and C on V_s are shown in Fig. 10, where each labeled line corresponds to the series of similarly labeled peaks in the spectra (Fig. 5). Series A and C define straight lines. Because of the complexity of the B series (Fig. 5) I originally drew straight line B (Fig. 10) for just the three points corresponding to the steps observed for the highest V_s values. In that case the slopes of the straight lines are 7.1×10^{-2}, 1.7×10^{-2}, and 1.0×10^{-2}, for A, B, and C, respectively. An acceptable model should predict this dependence.

I suggest that the ground potential surface regions are due to an isolated positive charge, consisting of a surface hole and one or more surface excitons which formed in the beam landing area and diffused from there. An electric field will be set up between this positive charge and negative charge within the silicon. An electron entering this field will be accelerated to the surface until it gets close enough to emerge into the vacuum, ionizing an exciton as it does so. In this process of forming surface holes one electron ends up in the vacuum with essentially zero kinetic energy (peak X), the other in a vacuum state with an energy necessary for overall conservation and contributing to peak A, B, or C. Some of these processes are depicted in Fig. 9(c).

In the above process an outgoing electron will emerge into the vacuum when it has sufficient overlap with a vacuum state. In a strong electric field the spatial extent of a conduction electron wave packet is small. This wave packet has the form of a Bloch function multiplied by a Gaussian.[31] The location of the electron can be determined only to within a wavelength ($\lambda=2\pi/k$), so the electron will certainly emerge into the vacuum when it is at a distance λ from the surface. To proceed further it is necessary to make assumptions about the electric field. I assume a charge distribution that has the symmetry of the surface, i.e., planar, and note that the only distance scale normal to the surface is the thickness of the electron-hole sheath, t, of 600 A. The potential drop V_s will occur across distance t. The outgoing electron will be in a field of strength V_s/t, and will have an energy $\lambda V_s/t-a_i$ at distance λ from the surface, i.e., on emergence, where a_i is the binding energy of state i relative to the vacuum in the field-free case. The outgoing electron loses 2.9 eV in ionizing the exciton, and so is left with an energy E (eV),

$$E=eV_s\lambda/t-a_i-2.9\ . \tag{2}$$

This model predicts that a plot of E/e (V) versus V_s (V) will yield a straight line with slope (λ/t), and intercept $-(2.9+a_i)$ (V). The model predictions are discussed with the aid of the conduction-band structure for silicon (Fig. 10, inset),[32] in which energies are related to the top of the valence band, in turn related to the vacuum level.[16] I use Eq. (2) to deduce a_i and λ from the lines A, B, and C (Fig. 10), and locate the resulting states as circles on the band dispersion curves of Fig. 10 (inset).

There is a continuum of states in the relevant region of the bulk E versus k dispersion curves for silicon, with a corresponding continuum of binding energies, a_i (Fig. 10, inset). Electrons in certain types of states would not be expected to persist in high electric fields, however. In particular, electrons in states with low effective mass would be accelerated rapidly out of these states. Thus the probability of observing electrons emerging from such states is low. Conversely, electrons in states with high effective masses, at flat band regions or inflection points, for example, would resist acceleration out of these states. There would be a higher probability for seeing electrons emerging from such states in the sample, and observed peaks A, B, and C should consist of electrons emerging from such states.

States located at the points A, B, and C in Fig. 10 (inset) have high effective masses, and would be expected to persist in the high electric field, as noted above. For low values of V_s the B peak locations (Fig. 5) do not fit on the straight line B of Fig. 10. However, using Eq. (2) a line representing the high effective-mass states at B' in Fig. 10 (inset) can be plotted on Fig. 10, labeled B'. It is found that some B peaks for low values of V_s (Fig. 5) plot on this line (Fig. 10). Electrons emerging from states to the right of B in Fig. 10 (inset) can have a range of energies, and hence give the steplike appearance of peaks B, for $V_s<-200$ V, in the spectra (Fig. 5).

The model is not without an adjustable parameter, although it has been presented as such for simplicity. In practice the value of "t" deduced from the mean free path data has some uncertainty associated with it. The

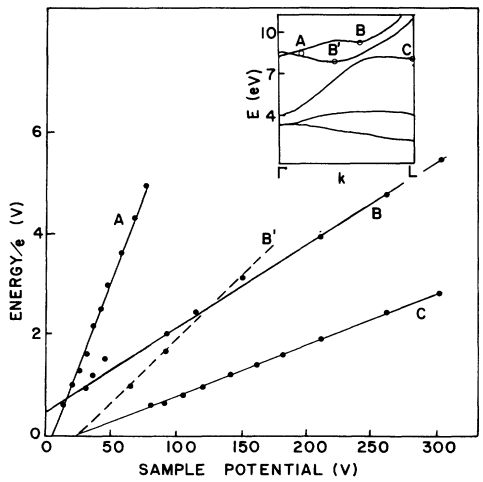

FIG. 10. The energy dependence of peaks A, B, and C on sample potential. Inset: Portion of the bulk band structure of silicon for the direction perpendicular to the (111) surface, Ref. 32. The circles are points deduced from the data of the main part of this figure by the model described in the text.

value was chosen so as to position point C on the Brillouin-zone boundary in Fig. 10 (inset). No other parameter was adjusted, and the quantitative agreement between the model predictions and the data is the main support for the model.

The model can qualitatively account for the other observed features. A reduced spectrum (Fig. 3) is invariably accompanied by an X peak, which was shown above to have a surface origin. The simplest explanation for the large reduction in secondary current is in terms of scattering of outgoing electrons by surface excitons in a manner similar to that discussed above for the X to C peaks. An important difference is that for $V_s=0$ the wave packet of the electron in the bulk conduction state will be extended, and will have greater spatial overlap with other band states than for the outgoing electron in the high electric-field region, $-12<V_s<-300$ V. In this case scattering to crystal states, from which emergence into the vacuum is impossible, becomes more probable. The surface exciton would still be ionized, with the ejected electron contributing to peak X, but the would-be emergent band electron would no longer be scattered into vacuum states, i.e., peaks A, B, and C would not be observed. Overall, then, it is postulated that the presence of surface excitons is required to explain all of the unusual features observed in SEES.

I will describe one hypothesis for the reappearance of spectra of standard shape with increased n-type doping and with negative applied sample bias V_s. It was described above how surface exciton formation will always compete for surface holes in a secondary-emission experiment. The hypothesis for the reappearance of spectra of standard shape is based on processes which remove surface holes in competition with surface exciton formation. Promotion of these competing processes reduces surface exciton formation, leading to spectra of standard shape. The only process we need consider here is the recombination of electrons near the bottom of the bulk conduction band with surface holes. For the low-resistivity n-type samples there is an abundance of conduction electrons to recombine with surface holes. The surface will be n type, and standard spectra will result.

For a sufficient concentration of bulk holes in a p-type sample there will be a loss of conduction electrons near the surface by recombination. Surface holes will be available to form surface excitons, subsequently reducing the secondary current. With sufficiently negative V_s applied to a p-type sample, low-energy conduction electrons due to the incoming beam will be attracted to the surface, making it n type and restoring the standard spectrum (Fig. 4). In this case, however, it must be postulated that there is still some formation of surface excitons. To account for the X, A, B, and C peaks these excitons must be repelled from the n-type surface region.

The dependence of SEES on incoming angle (Fig. 7) can be explained in a similar fashion. For angles closer to grazing incidence the primary electrons end up in the conduction band near the surface [Fig. 9(b)]. These electrons compete for surface holes, reducing surface exciton formation, and again leading to SEES with shapes more similar to the standard shape. Another factor could be important in this case; that is, the ionization of surface excitons by high-energy incoming electrons with a velocity component parallel to the surface.

The ELS of Fig. 8 are also cited as supporting the model. It was postulated that an incident beam could form surface excitons as described above, and also act as the probe beam in an ELS experiment to directly observe the ionization loss process put forward in the model. Two broad loss peaks are observed, at 3.0 ± 0.4 and 9.2 ± 0.4 eV, respectively. At the angles of incidence and scattering involved it is highly probable that the losses are the results only of surface processes. A loss peak due to bulk processes has also been observed at an energy close to 3 eV.[23] That peak is much narrower than the one reported here. I suggest that the 3-eV loss is due to the ionization of surface excitons, in a process similar to that responsible for peaks X to C, described above.

With certain assumptions an estimate of the lifetime of these surface excitons can be made. To explain the nearly complete reduction of the low-energy region of the SEES for the p-type sample I will assume an equilibrium density of one exciton per unit cell of the reconstructed, 7×7, surface. In the beam landing region of area A there would be A/a excitons, where a is the area of the reconstructed unit cell. I assume that a sufficient supply of surface holes exists on the p-type surface so that the production rate of surface excitons is limited by the arrival rate at the surface, from within, of electrons with energies greater than 2.5 eV above the top of the valence band. The arrival rate of these electrons, per incident 70-eV electron, was estimated from the mean-free-path data in the literature,[27–29] using a Monte Carlo method. This arrival rate was equated to the number of surface excitons decaying per second, DA/a, where D is the decay rate. Observation of reduced spectra with an incident-beam current of 2×10^{-9} A then leads to an estimated half-life, $0.69/D$, of order 0.1 s. Contrast this with the 2-μs lifetime estimated from the ELS (Ref. 22) by the method described by Froitzheim, Ibach, and Mills.[33] The excitons observed indirectly in the SEES apparently differ in lifetime from those observed in ELS. I can suggest one reason why two otherwise identical surface excitons could have widely differing lifetimes. The excitons formed in ELS are singlet states in that the excited electron has the same spin as the hole it left behind. In the mode of formation suggested for the excitons on the p-type surface the captured electrons can have spin parallel or antiparallel to the hole. The parallel spin excitons would decay rapidly, leaving the triplet states as the long-lived ones responsible for the observations reported here. The estimated half-life of >0.1 s is unusually long. No calculations have been made of the wave functions of these surface excitons, so nothing theoretical is known about the lifetime. The (111)7×7 surface consists of triangular islands separated by channels.[34] A viable model for the surface exciton has the hole on an island, surround by an electron which spends most of its time in the channels.[35]

With such a huge effect on the SEES it might be expected that the presence of surface excitons would manifest itself in other electron-scattering experiments. I have

investigated the literature of surface-sensitive core spectroscopies involving the silicon L state, considering what effects that the constituents of surface excitons might have on features in ELS, Auger, and appearance potential spectra (APS). Because it would be at an energy where there is no other contribution to the Auger spectra, the most propitious feature to look for in the Auger spectrum would be a high-energy feature arising from transitions of selvedge electrons to a core hole. However, if the selvedge state wave functions in silicon are anything like those at metal surfaces they will overlap little with core states of surface atoms.[36] I have found no experimental evidence for such a feature in the Auger spectrum. For core-state excitations observed in absorption spectroscopies, ELS and APS, the feature to look for would be a preedge peak due to the excitation of a $2p$ electron into the hole of a surface exciton. Such a peak would lie outside the normal $2p$ excitation spectrum. Features due to surface excitons would be expected to appear for p-type samples and for high-resistivity n-type samples, but not for low-resistivity n-type samples. Koma and Ludeke saw no precursor peak in the ELS from the (111)7×7 surface of 5-Ω cm n-type silicon.[37] However, Margaritondo and Rowe did see such a precursor peak to the main edge, although in a sample of unspecified resistivity.[38] They characterized the feature as a giant surface core exciton, in which a state from the bottom of the surface conduction band is pulled to below the top of the valence band by the core hole. I suggest that the feature is due to excitations of $2p$ electrons to surface exciton holes. If this is the case the feature would vanish when a sufficiently negative potential is applied to the sample. The success of this prediction rests specifically on the presence of long-lived surface excitons. My apparatus, with its low beam current and 1° collection angle, is not suitable to test the suggestion because of the high signal-to-noise ratio needed for this experiment. Because of its nature, the APS experiment would be more difficult to implement to test the suggestion.

Whenever there is a bare hole at this surface there will be a vacant state at 2.9 eV below the vacuum level, the acceptor state for the exciton electron. This state should be observed in all experiments which probe empty surface states. Tunneling spectroscopy is such an experiment. The sample-tip bias necessary to probe vacant states attracts surface holes. Becker *et al.* did see a peak in the tunneling conductance spectra on p-type silicon at a binding energy of 2.95±0.15 eV below the vacuum level, when averaged over a unit cell.[39] I suggest that this peak is due to the formation of surface excitons: the binding energy is appropriate. Occupied states are detected in tunneling spectroscopy when the sample-tip bias is reversed from the above case, and the tip Fermi level is below the energy level of the occupied state. The presence of surface excitons would be detected as a peak in this spectrum at the same binding energy as in the exciton formation experiment. This raises the possibility of two tips "communicating" with each other.[35]

The same state as detected in tunneling spectroscopy is observed in inverse photoemission,[39,40] although the doping type of this sample was not identified in that work.[40] The peak seen at the appropriate energy in the inverse photoemission experiment for the (111)7×7 surface is not seen on the silicon (100)2×1 surface.[40]

These experiments are often done with the electron emitter and the sample arranged in simple diode fashion. This configuration precludes the variation of a sample-environment bias independent of the cathode-sample potential difference. However, the inverse photoemission experiment can be done with an electron gun source.[41] In that case holes can be removed from the surface by applied potential, as in the SEES experiment. Another prediction of the model, then, is that the relevant peak in the inverse photoemission experiment will disappear when surface holes are removed from the silicon (111)7×7 surface by applied bias. This experiment would serve to identify the excitonic nature of the final state, independent of its lifetime.

Excitons on this surface have received little study in the past. In the present work the primary electron indirectly responsible for the formation of an exciton need not be the same as that indirectly responsible for its decay. The two primary electrons could be viewed as exciton forming and exciton probing, respectively. Other probes could also be used.[35] I suggest that firing a beam of electrons with energy between 40 and 300 eV at a 10-Ω cm p-type Si (111)7×7 surface will result in the presence of surface excitons in and around the beam landing area. In a similar fashion long-lived excitons can be formed by electrons tunneling from a field-emitter tip to the surface. These surface exciton sources should facilitate their study.

Apart from possible applications of tips communicating with each other,[35] as mentioned above, there are possible interactions of long-lived surface excitons with electrical conductivity,[35,42,43] surface reconstruction[35,44] and epitaxial film growth,[35] and optical phenomena.[35]

V. SUMMARY AND CONCLUSIONS

The main experimental results reported here are the unusual SEES from p-type silicon (111)7×7 surfaces. The secondary current is reduced, and the shape of the spectra cannot be understood on the standard model which was developed for metal samples, and which applies to low-resistivity n-type samples. With sufficiently negative potential applied to the p-type samples, SEES with the standard shape are recovered, but another unusual feature appears; that is, secondary electrons are observed with energies below that of the nominal vacuum level of the sample. This behavior is only possible for nonmetallic samples, of course.

In developing a model for the observations, a method of formation of surface excitons was postulated for this surface: electrons diffracted from the bulk into the selvedge region are trapped by surface holes to form excitons. In the interpretation presented here the surface excitons are attracted to surface holes in a p-type surface and repelled by surface electrons in an n-type surface. The surface excitons were observed in a region outside of the beam landing area in which they were presumably formed, demonstrating their mobility.

Surface excitons apparently come in singlet and triplet

states. Their formation has been observed in four experiments. They are formed by direct excitation in ELS, as in Ref. 22, and by the trapping of an electron incident from the vacuum by a surface hole, as in the two probes of vacant states, tunneling spectroscopy, and inverse photoemission. Both singlet and triplet states can be formed in these processes. Finally, surface excitons can be formed by the trapping of electrons incident from within the sample, as demonstrated in the SEES results presented here.

Other than by observing their formation, the presence of surface excitons has been detected in SEES, ELS (Fig. 8), and possibly core-state ELS. In each case it is the long-lived, triplet variety which is detected.

ACKNOWLEDGMENTS

The apparatus was skillfully constructed by T. Swol. Helpful discussions with F. Szmulowicz, S. Thurgate, H. L. Grubin, G. A. Peterson, R. A. Bartram, Y. Hahn, P. B. Sewell, and M. Dorota are acknowledged. I am grateful to J. E. Northrup for permission to use the band structure in the Fig. 10 inset, and acknowledge sample donations from Motorola Corp. and financial assistance from the University of Connecticut Research Foundation. The spectra from the 100 Ω cm *n*-type sample were measured in a program supported by NSF Grant No. DMR 8000022.

[1]M. Rossler and W. Brauer, in *Particle Induced Electron Emission I,* edited by G. Hohler, Springer Tracts in Modern Physics Vol. 122 (Springer-Verlag, Berlin, 1991), and references therein.
[2]A. R. Shul'man, Y. A. Morozov, and V. V. Korablev, Fiz. Tverd. Tela (Leningrad) **11**, 1360 (1969) [Sov. Phys. Solid State **11**, 1101 (1969)].
[3]K. Goto and K. Ishikawa, J. Appl. Phys. **43**, 1559 (1972).
[4]K. Goto and K. Ishikawa, J. Appl. Phys. **44**, 132 (1973).
[5]P. E. Best, Phys. Rev. Lett. **34**, 674 (1975).
[6]P. E. Best, Phys. Rev. B **14**, 606 (1976).
[7]P. E. Best, Phys. Rev. B **19**, 2246 (1979).
[8]O. M. Artamonov, A. G. Vinogradov, and A. N. Terehkov, Izv. Akad. Nauk. SSSR, Ser. Fiz. **52**, 1578 (1988) [Bull. Acad. Sci. USSR, Phys. Ser. **52**, 107 (1988)].
[9]G. V. Hansson and R. I. Uhrberg, Surf. Sci. Rep. **9**, 197 (1988).
[10]P. E. Best, Rev. Sci. Instrum. **46**, 1517 (1975).
[11]P. E. Best, Rev. Sci. Instrum. **48**, 696 (1977).
[12]R. C. Henderson, J. Electrochem. Soc. **119**, 772 (1972).
[13]J. R. Vig, J. Vac. Sci. Technol. A **3**, 1027 (1985).
[14]F. Szmulowicz, Phys. Rev. B **23**, 1652 (1981).
[15]C. Davisson and L. H. Germer, Phys. Rev. **24**, 666 (1924).
[16]F. J. Himpsel, G. Hollinger, and R. A. Pollak, Phys. Rev. B **28**, 7014 (1983).
[17]N. R. Whetten, in *Methods of Experimental Physics,* edited by V. W. Hughes and H. L. Schultz (Academic, New York, 1967), Vol. 4A, p. 69.
[18]L. R. Koller and J. S. Burgess, Phys. Rev. **70**, 571 (1946).
[19]T. E. Everhart, O. C. Wells, and R. K. Matta, J. Electrochem. Soc. **111**, 929 (1964).
[20]R. M. Broudy, Phys. Rev. B **3**, 3641 (1971).
[21]J. E. Rowe and H. Ibach, Phys. Rev. Lett. **31**, 102 (1973).
[22]P. E. Best, Phys. Rev. B **12**, 5790 (1975).
[23]S. Hasegawa, H. Iwasaki, M. Akizuki, S. T. Li, and S. Nakamura, J. Vac. Sci. Technol. A **4**, 2336 (1986).
[24]S. Hasegawa, H. Iwasaki, S. T. Li, and S. Nakamura, Phys. Rev. B **32**, 6949 (1985).
[25]H. Kobayashi, K. Edamoto, M. Onchi, and M. Nishijima, Solid State Commun. **44**, 1449 (1982).
[26]P. S. Wei and A. W. Smith, Surf. Sci. **27**, 675 (1971).
[27]S. Tanuma, C. J. Powell, and D. R. Penn, J. Vac. Sci. Technol. A **6**, 1041 (1988).
[28]S. Tanuma, C. J. Powell, and D. R. Penn, Surf. Interf. Anal. **17**, 911 (1991).
[29]E. O. Kane, Phys. Rev. **159**, 624 (1967).
[30]P. A. Wolff, Phys. Rev. **95**, 56 (1954).
[31]W. A. Harrison, *Solid State Theory* (Dover, New York, 1979), p. 64.
[32]W. B. Jackson, J. E. Northrup, J. W. Allen, and R. I. Johnson, Phys. Rev. Lett. **56**, 1187 (1986); J. E. Northrup (private communication).
[33]H. Froitzheim, H. Ibach, and D. L. Mills, Phys. Rev. B **11**, 4980 (1975).
[34]K. Takayanagi, Y. Tanishira, M. Takahashi, and S. Takahashi, J. Vac. Sci. Technol. A **3**, 1502 (1985).
[35]P. E. Best (unpublished).
[36]E. G. McRae, Rev. Mod. Phys. **51**, 541 (1979).
[37]A. Koma and R. Ludeke, Phys. Rev. Lett. **35**, 107 (1975).
[38]G. Margaritondo and J. E. Rowe, Phys. Lett. **59A**, 464 (1977).
[39]R. S. Becker, J. A. Golovchenko, D. R. Hamann, and B. S. Swartzentruber, Phys. Rev. Lett. **55**, 2032 (1985).
[40]F. J. Himpsel and Th. Fauster, J. Vac. Sci. Technol. A **2**, 815 (1984).
[41]Th. Fauster, F. J. Himpsel, J. J. Donelon, and A. Marx, Rev. Sci. Instrum. **54**, 68 (1983).
[42]D. Allender, J. Bray, and J. Bardeen, Phys. Rev. B **7**, 1020 (1973).
[43]Ginzburg, Usp. Fiz. Nauk **101**, 185 (1970) [Sov. Phys. Usp. **13**, 335 (1970)].
[44]J. C. Phillips, Surf. Sci. **40**, 459 (1973).